

Supporting Information: Quantifying Polaron Densities in Sequentially Doped Conjugated Polymers: Exploring the Upper Limits of Molecular Doping and Conductivity

Tucker L. Murrey,^{*,†,‡} Melissa Berteau-Rainville,[¶] Goktug Gonel,[§] Jan Saska,^{||}
Nikolay E. Shevchenko,^{||} Alice S. Ferguson,^{§,#} Rachel M. Talbot,[§] Nichole L.
Yacoub,[§] Fengyu Zhang,[‡] Antoine Kahn,[‡] Mark Mascall,^{||} Ingo Salzmänn,[⊥] and
Adam J. Moule^{*,§}

[†]*Department of Material Science and Engineering, University of California, Davis, CA,
USA*

[‡]*Department of Electrical and Computer Engineering, Princeton University, Princeton,
NJ, USA*

[¶]*Institut National de la Recherche Scientifique (INRS), Centre Energie Materiaux
Telecommunications, Varennes, QC, Canada*

[§]*Department of Chemical Engineering, University of California, Davis, CA, USA*

^{||}*Department of Chemistry, University of California, Davis, CA, USA*

[⊥]*Department of Physics, Department of Chemistry & Biochemistry, Concordia University,
Montréal, QC, Canada*

[#]*Current address: Department of Chemical and Biological Engineering, Princeton
University, Princeton, NJ, USA*

E-mail: tlmurrey@ucdavis.edu; amoule@ucdavis.edu

Phone: +1 (530) 754-8669

Θ Derivation

First we define the integrated absorption per site as α_P for polaron sites and α_n for neutral sites,

$$\int_{0eV}^{4eV} A_P d\nu = \alpha_P N_P \quad (S1)$$

$$\int_{0eV}^{4eV} A_n d\nu = \alpha_n N_n \quad (S2)$$

with N_P and N_n representing total polaron and neutral sites respectively. Next, we define the polaron mole fraction, Θ , as the number of polaron sites over the total sites and equate to the integrated absorbance.

$$\Theta = \frac{N_P}{N_P + N_n} = \frac{\frac{1}{\alpha_P} \int_{0eV}^{4eV} A_P d\nu}{\frac{1}{\alpha_P} \int_{0eV}^{4eV} A_P d\nu + \frac{1}{\alpha_n} \int_{0eV}^{4eV} A_n d\nu} \quad (S3)$$

We then condense the expression to obtain Equation S4.

$$\Theta = \frac{\int_{0eV}^{4eV} A_P d\nu}{\int_{0eV}^{4eV} A_P d\nu + \frac{\alpha_P}{\alpha_n} \int_{0eV}^{4eV} A_n d\nu} \quad (S4)$$

Next we need to obtain $\frac{\alpha_P}{\alpha_n}$ to account for differing extinction coefficients for neutral and polaronic states. We start by defining, $\bar{\Delta}$, as the change in the total neutral and polaron absorbance integrals normalized by the absorbance of the neutral polymer film.

$$\bar{\Delta} = \frac{\int_{0eV}^{4eV} A_P d\nu + \int_{0eV}^{4eV} A_n d\nu - \int_{0eV}^{4eV} A_n^0 d\nu}{\int_{0eV}^{4eV} A_n^0 d\nu} \quad (S5)$$

Reorganize Equation S5, and plug in Θ .

$$\bar{\Delta} = \frac{\alpha_P N_P + \alpha_n N_n - (N_P + N_n) \alpha_n}{(N_P + N_n) \alpha_n} = \frac{N_P}{N_P + N_n} \cdot \frac{\alpha_P - \alpha_n}{\alpha_n} = \Theta \cdot \frac{\alpha_P - \alpha_n}{\alpha_n} \quad (S6)$$

Now rearrange for $\frac{\alpha_P}{\alpha_n}$.

$$\frac{\alpha_P}{\alpha_n} = \frac{\bar{\Delta}}{\Theta} + 1 \quad (\text{S7})$$

Finally insert Equation S7 into Equation S4 and reorganize for Θ .

$$\Theta = \frac{\int_{0\text{eV}}^{4\text{eV}} A_P d\nu}{\int_{0\text{eV}}^{4\text{eV}} A_P d\nu + \left(\frac{\bar{\Delta}}{\Theta} + 1\right) \int_{0\text{eV}}^{4\text{eV}} A_n d\nu} \quad (\text{S8})$$

$$\Theta = \frac{\int_{0\text{eV}}^{4\text{eV}} A_P d\nu - \bar{\Delta} \cdot \int_{0\text{eV}}^{4\text{eV}} A_n d\nu}{\int_{0\text{eV}}^{4\text{eV}} A_P d\nu + \int_{0\text{eV}}^{4\text{eV}} A_n d\nu} = \frac{\int_{0\text{eV}}^{4\text{eV}} A_P d\nu - \eta}{\int_{0\text{eV}}^{4\text{eV}} A_P d\nu + \int_{0\text{eV}}^{4\text{eV}} A_n d\nu} \quad (\text{S9})$$

Note, if $\frac{\alpha_P}{\alpha_n} = 1$, then $\bar{\Delta} = 0$. $\bar{\Delta}$ is obtained for a given polymer using a linear fit to Figure S1. $\bar{\Delta}$ provides a correction factor to account for different extinction coefficients in polaron vs neutral absorbance spectra.

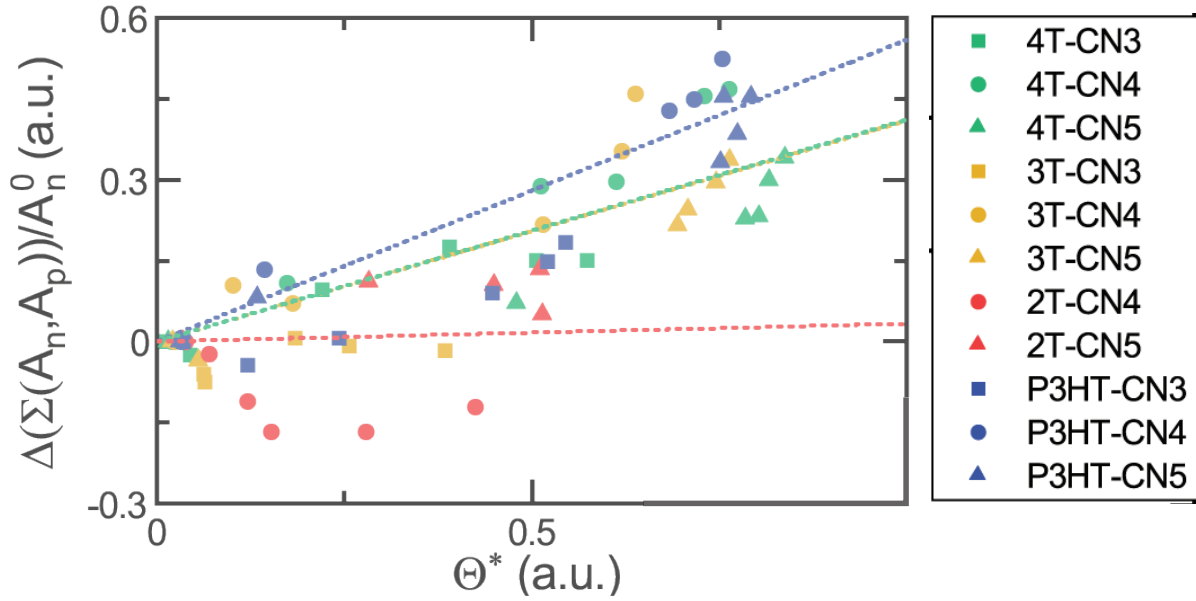


Figure S1: Change in total absorbance $\frac{\Delta(\Sigma(A_n, A_p))}{A_n^0}$ as a function of the uncorrected polaron mole fraction Θ^* . Dotted lines indicate a linear fit to the data from each polymer (for all dopants). The slope of this line is the increase in total integrated absorbance with increased doping level.

UV-vis-NIR Gaussian Fits

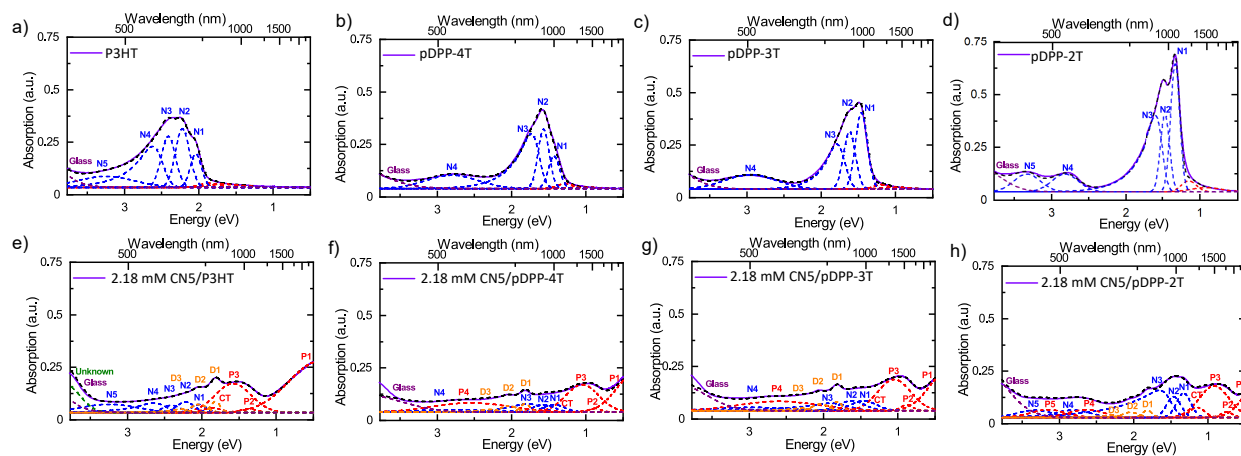


Figure S2: Cumulative Gaussian fits to UV-vis-NIR of a) P3HT, b) pDPP-4T, c) pDPP-3T, and d) pDPP-2T films and e) f) g) h) the same films doped from a 2.18mM CN5/acetonitrile solution.

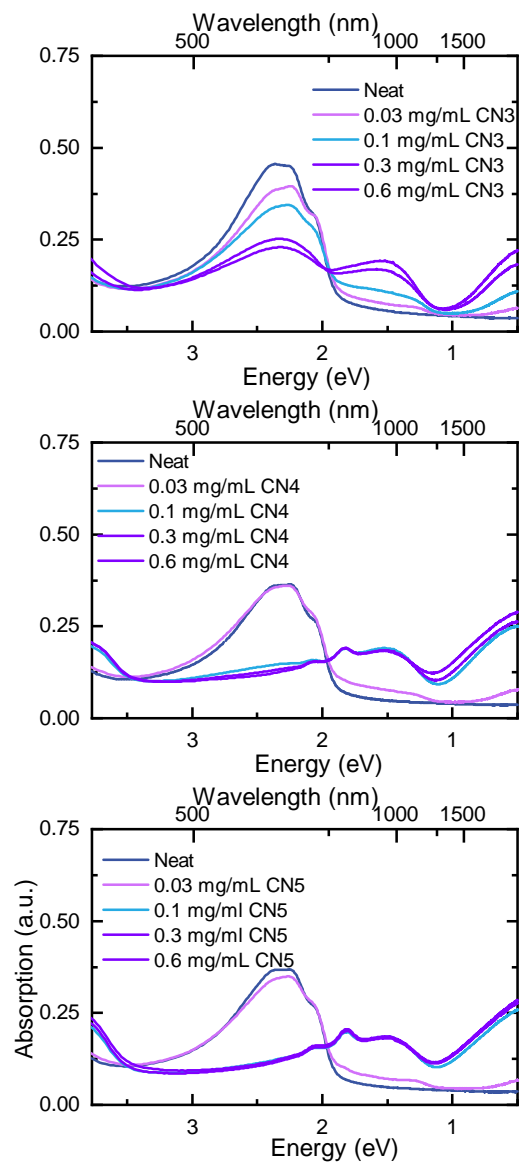


Figure S3: UVvis of P3HT films exposed to various concentrations of CN3 (top), CN4 (middle), CN5 (bottom).

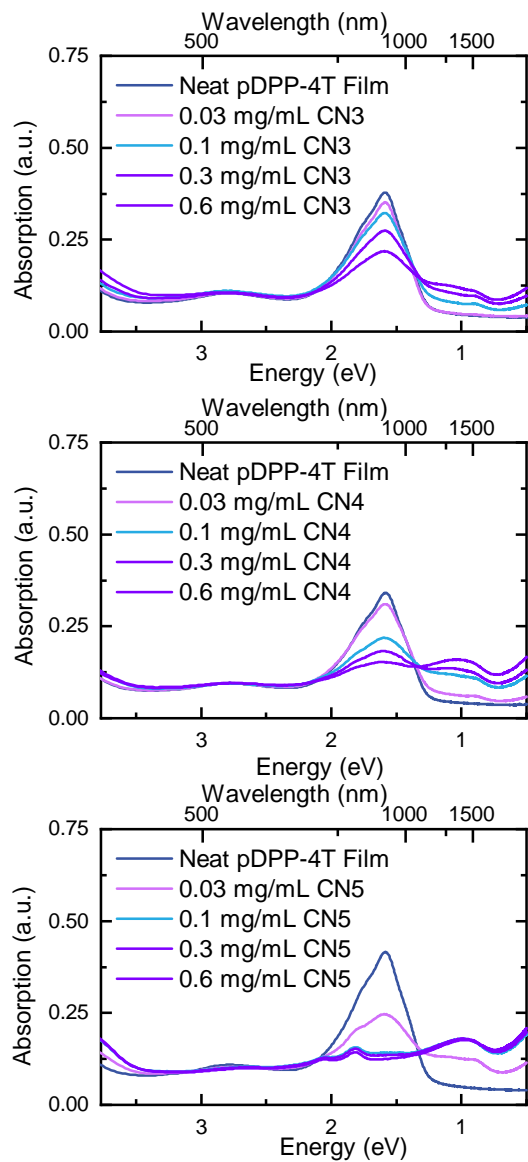


Figure S4: UVvis of pDPP-4T films exposed to various concentrations of CN3 (top), CN4 (middle), CN5 (bottom).

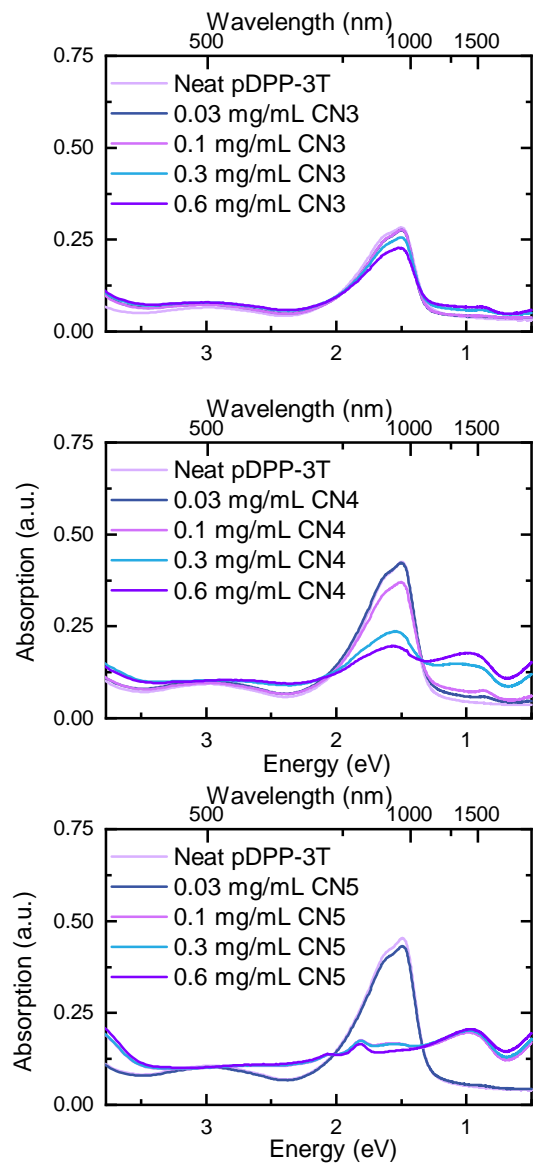


Figure S5: UVvis of pDPP-3T films exposed to various concentrations of CN3 (top), CN4 (middle), CN5 (bottom).

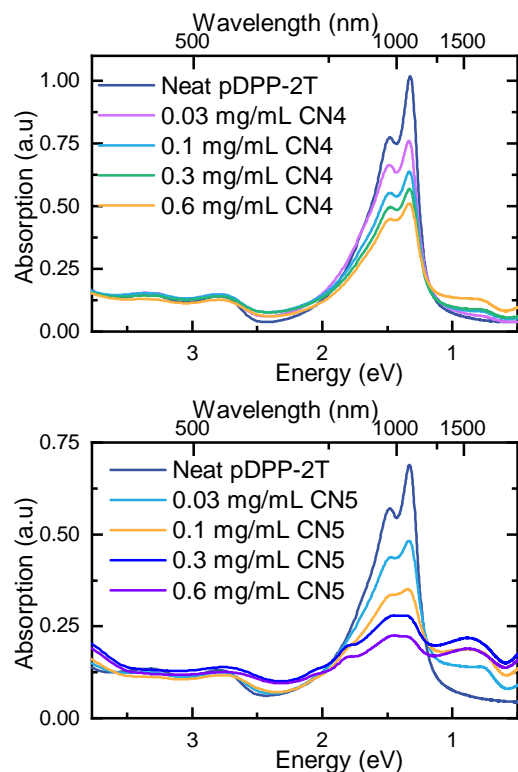


Figure S6: UVvis of pDPP-2T films exposed to various concentrations of CN4 (top), CN5 (bottom).

Fitting of the UV-Vis-NIR spectra followed a procedure demonstrated previously for P3HT doped with F4TCNQ.¹ The model and procedure are detailed here and in our 2022 Advanced Electronic Materials publication.² An example of a neutral and doped fit spectrum for each polymer with labeled Gaussian peaks is given in Figure S2.

P3HT is fit with a series of three narrow vibronic peaks labeled N1–N3 ($A_{0-0} - A_{0-3}$) that represent the ordered/crystalline sites in P3HT. A fourth anharmonic peak, labeled N4, is included as a superposition of higher order harmonic peaks. A broad absorbance centered at 3.25 eV represents the amorphous sites in P3HT. All of the peaks in P3HT are Gaussian.

All of the DPP polymers were best fit with a series of two narrow harmonic peaks labeled N1, N2. A third anharmonic peak, labeled N3, is included as a superposition of higher order harmonic peaks. The pDPP-4T and pDPP-3T polymers also have a broad absorbance centered around 2.8 eV and 3.0 eV, respectively, that represents absorbance

from the individual monomeric units on the backbone. The pDPP-2T polymer has peaks at 2.77 eV and 3.35 eV that represent the same A-A and D-D absorbances as in the pDPP-3T and pDPP-4T samples.

For all four polymers, the polaron spectrum is fit with a series of three peaks. The P1 peak, also known as the “B” peak, is centered at 0.33 eV for all three DPP polymers for the fitting. The P3HT polymer has the P1 peak at 0.42 eV. For all spectra, the P1 peak is centered off of the edge of the UV-Vis-NIR spectrum, which complicates fitting. The peak width of the P1 peak increased with doping level for all four polymers.

The P2 peak is best seen at low doping levels. For many of the 0.03 and 0.1 mg/mL solution concentrations, there is a pronounced lower energy polaron peak (0.75 eV for DPP-2T, 0.88 eV for DPP-3T and DPP-4T and 1.37 eV for P3HT). The width of the P2 peak is fixed throughout.

The P3 peak overlaps the neutral absorbance for every polymer. This peak is centered at 0.92 for DPP-2T, 1.05 for DPP-3T, 1.05 for DPP-4T, and 1.58 for P3HT. The width of the P3 peak is fixed throughout.

The dopant anion is fit with a series of two symmetric and one asymmetric Gaussian peaks. The fit to a solution of $\text{CN6-CP}^-\text{K}^+$ in ACN is depicted in². The ratio of the three anion peaks are fixed for all spectra. The ratio between the sum of the P1, P2, and P3 peak areas and the anion peak areas are also fixed for each given dopant species.

Spectral Fitting Rules for the DPP polymers:

1. All peaks are Gaussian except N3, which is a superposition of several higher order vibronic transitions. It is modeled as an asymmetric Gaussian that broadens to the blue.
2. At a given doping level $W_{N1}=W_{N2}=W_{N3}$.
3. As the doping level increases $W_{N1}=W_{N2}=W_{N3}$ increases.

4. The separation distance (S) between N1 and N2 is equal to twice the width of N1 in the neat film ($S_{N1-N2} = 2 \times W_{N1}$).
 - (a) *Except:* pDPP-2T, $S_{N1-N2} \approx 2 \times W_{N1}$
5. The separation distance (s) between N2 and N3 is equal to the width of N1 in the neat film ($S_{N2-N3} = W_{N1}$).
6. As the doping level increases, N3 becomes increasingly broadened to the blue.
7. The ratio of the areas of the neutral high energy DD-AA peak(s) (peaks N4 and N5 in pDPP-2T, peak N4 in pDPP-3T and pDPP-4T) over the sum of the areas of N1, N2, and N3 is held constant regardless of doping level. ie $\frac{\sum(N4,N5)}{\sum(N1,N2,N3)} = Constant$.
8. For every high energy DD-AA peak there exists a high energy polaron peak (peaks P4 and P5 in pDPP-2T, peak P4 in pDPP-3T and pDPP-4T).
9. The width of the high energy DD-AA polaron peak(s) is(are) equal to the width of the high energy DD-AA peak(s) at a given doping level.
10. The width of the high energy DD-AA neutral and polaron peak(s) increase(s) with doping level.
11. The high energy DD-AA polaron peak(s) is(are) red shifted from their respective neutral high energy peak(s) by twice the width of the neutral high energy DD-AA peak in the neat polymer samples.
12. The area of the high energy DD-AA polaron peak(s) is (are) determined by Θ and the area of the neutral DD-AA peak(s) so that $\Theta = \frac{\sum(P4,P5)}{\sum(P4,P5,N4,N5)}$
13. There are three dopant anion peaks. The three widths and peak centers and the asymmetry of the third dopant peak are estimated from the fit to CN6-CPK salt and kept constant across all samples.

14. The ratios of the dopant peak areas are kept constant across all samples. $\frac{D1}{D2} = 0.8$,
 $\frac{D1}{D3} = 1.45$

15. The ratio of the polaron peak areas over the dopant peak areas is kept constant for a given dopant species.

(a) CN3: $\frac{\sum(P1,P2,P3)}{D1} = 80$

(b) CN4: $\frac{\sum(P1,P2,P3)}{D1} = 80$

(c) CN5: $\frac{\sum(P1,P2,P3)}{D1} = 30$

Spectral Fitting Rules for P3HT:

1. All peaks are Gaussian, except N4, which is a superposition of several higher order vibronic transitions. It is modeled as an asymmetric Gaussian that broadens to the blue.
2. $W_{N1} < W_{N2} = W_{N3} = W_{N4} < W_{N5}$.
3. As the doping level increases W_{N1} and $W_{N2} = W_{N3} = W_{N4}$ increases.
4. The separation distance (S) between N1 and N2 is approximately twice the width of N1 in the neat film ($S_{N1-N2} \approx 2 \times W_{N1}$).
5. The separation distance (S) between N2 and N3 is equal to twice the width of N2 in the neat film ($S_{N2-N3} = 2 \times W_{N2}$).
6. The separation distance (S) between N3 and N4 is equal to the width of N2 in the neat film ($S_{N3-N4} = W_{N2}$).
7. As the doping level increases, N4 becomes increasingly broadened to the blue.
8. There exists a large Gaussian neutral amorphous peak (N5).

9. There are three dopant anion peaks. The three widths and three peak centers and the asymmetry of the third dopant peak are estimated from the fit to CN6-CPK salt and kept constant across all samples.
10. The ratios of the dopant peak areas are kept constant across all samples. $\frac{D1}{D2} = 0.8$, $\frac{D1}{D3} = 1.45$
11. The ratio of the polaron peak areas over the dopant peak areas is kept constant for a given dopant species.
 - (a) CN3: $\frac{\sum(P1,P2,P3)}{D1} = 100$
 - (b) CN4: $\frac{\sum(P1,P2,P3)}{D1} = 70$
 - (c) CN5: $\frac{\sum(P1,P2,P3)}{D1} = 40$

Determining the polymer ionization energy

There are two established methods for determining the ionization energy for semiconducting polymers. Cyclic voltammetry (CV) measures the change in current in an electrochemical cell as a function of the applied potential. CV provides oxidation and reduction information. For these samples the CV information was previously published.³ Since it is necessary to measure CV using a polar solvent (acetonitrile) we were concerned that the solvent environment could make the determination of the ionization energy less accurate for low doping concentrations.

In principle, ultraviolet photo-emission spectroscopy (UPS) provides a more accurate measurement of the ionization energy for a polymer film. Figure S7 shows the intensity vs energy for all four polymers on ITO substrates. Here we find that there is little difference between the ionization energies for the four polymers compared to the CV measurements and in addition UPS indicates a much lower ionization energy for the DPP polymers. Wegner et. al. recently published an article detailing that for simulation of doping experiments, CV measurements are more accurate than UPS because UPS measurements are very sensitive

to molecular orientation.⁴ We report the same finding here. P3HT and pDPP-4T have both been reported to stack predominantly end-on with respect to the polymer substrate, meaning that photoelectrons are ejected through the side chains of the polymer. By comparison, pDPP-2D has been reported to orient predominantly face-on to the substrate, which significantly alters the surface dipole and thereby reduces the effective ionization potential with respect to a polymer that is oriented end-on. For these reasons, only the CV data is considered for determination of the ionization energies in this publication. The UPS data is included here for completeness.

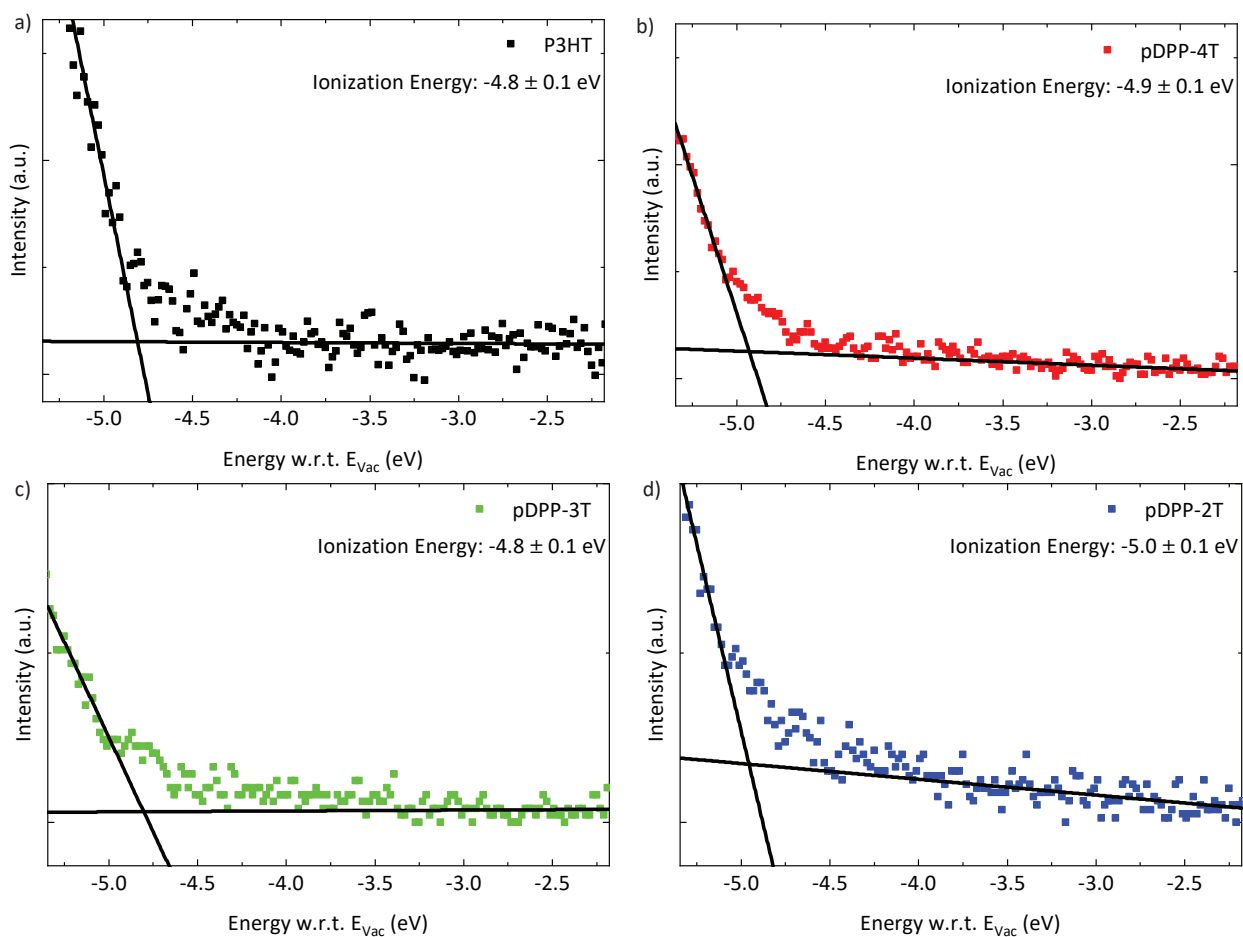


Figure S7: Ultraviolet photo-emission Spectroscopy of a) P3HT, b) pDPP-4T, c) pDPP-3T, and d) pDPP-4T films. Ionization Energy of each of the films is obtained through linear extrapolation of the highest molecular orbital in a P3HT film.

Maximum Charge Density Calculation

Figure 1 of the main text makes a calculation of the maximum possible polaron and later bipolaron density. This section details how that calculation was made. First the total number of sites per volume for each undoped polymer is calculated using:

$$\frac{\text{sites}}{\text{volume}} = \frac{\rho N_A}{M_W} \quad (\text{S10})$$

where ρ is the polymer density estimated to be $1.1 \frac{\text{g}}{\text{cm}^3}$, N_A is Avogadro's number and M_W is the molecular weight of the polymer. Table 1 of the main text lists the polaronic maximum as this site density. This calculation assumes that every site on the polymer contains one polaron and the anion has no volume. The same table determines the bipolaronic maximum with the assumption that every polymer site contains two polarons (or one bipolaron) and the counter ion has not volume. Clearly this ideal maximum cannot be reached and literature claiming higher charged densities should be discounted.

To determine a more realistic upper limit, it is necessary to make an estimate of the volume increase for a single site that includes the anion. Here we use ChemAxon MarvinSketch to estimate the Van der Waal volumes of the polymer sites and anions (Table S1). Admittedly this is a crude estimate of molar volume since the polymers and dopants assume a variety of molecular geometries. However, for simplicity, we assumed that the density of the samples were fixed at $1.1 \frac{\text{g}}{\text{cm}^3}$ for all samples. We hope that future publications will make careful measurements of density change with doping level for different polymers to reduce the uncertainty in this calculation. Figure 1c shows the percentage change in site volume assuming a 1:1 ratio of polymer sites to dopants, yielding a 25-40% increase in volume. Figure 1d shows the upper estimates of polaron density for a zero volume anion and for each of the three molecular dopants. Figure S8 shows both the polaronic and bipolaronic limits. The bipolaron calculation assumes that there are two holes and that there are two dopant counterions for each polymer site. This calculation shows that even assuming that every site

on the polymer is doubly charged, it is not possible to reach a hole density of $1 \times 10^{-21} \frac{g}{cm^{-3}}$ using these dopants because site density decreases due to volume expansion.

Polymer Site or Dopant	Van der Waal Volume (\AA^3)
P3HT	666.62
pDPP-4T	894.25
pDPP-3T	834.35
pDPP-2T	771.95
CN3	261.80
CN4	233.21
CN5	221.40

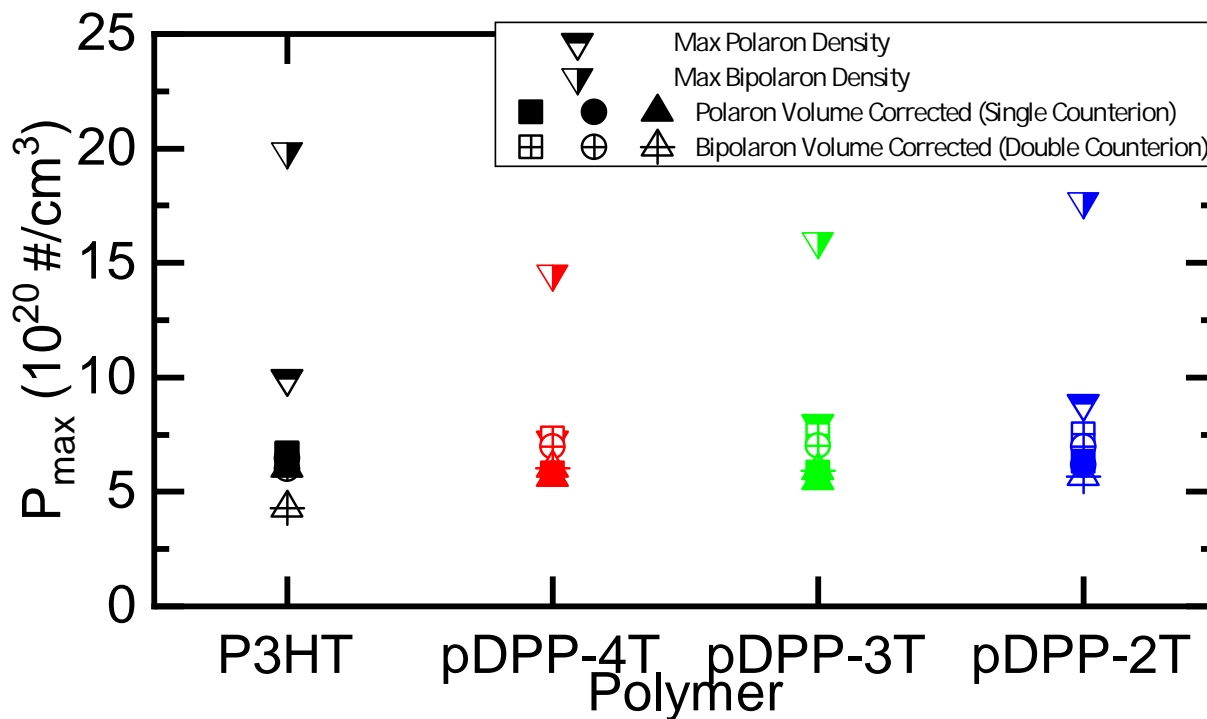


Figure S8: Estimates of the maximum polaronic and bipolaronic carrier densities for P3HT, pDPP-4T, pDPP-3T and pDPP-2T. Volume corrected maximum carrier densities for polarons and bipolarons assuming that the bipolaron occupies the same site as a polaron and accounting for the volume of a single or double counterion respectively.

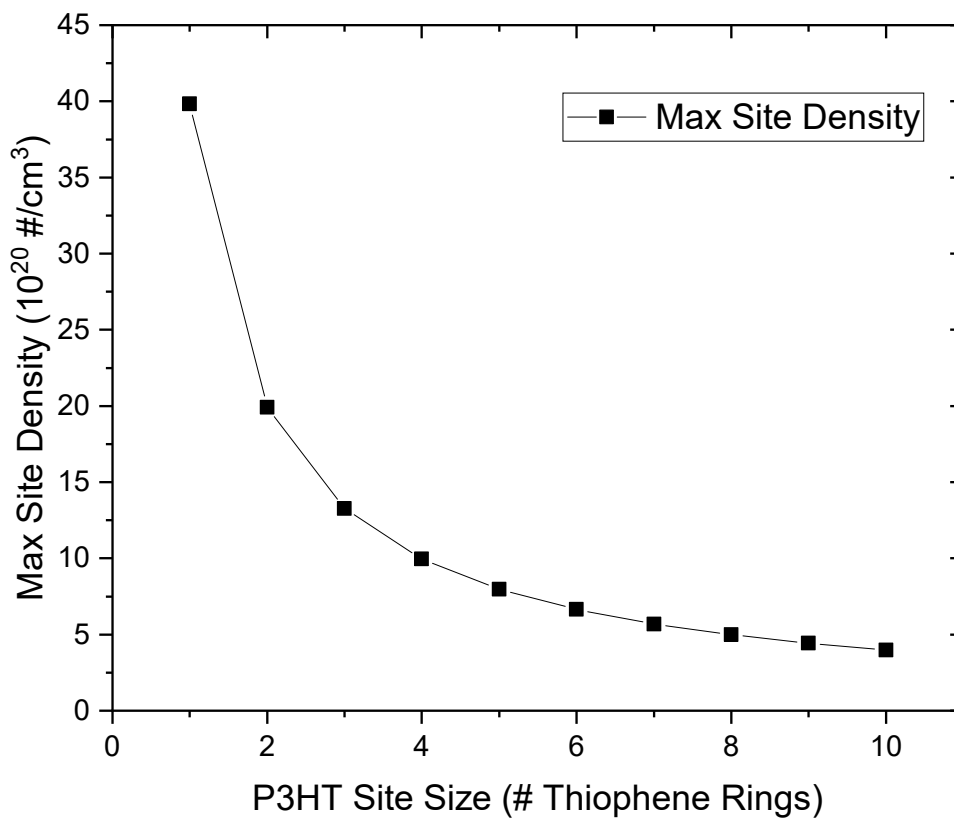


Figure S9: Estimates of the maximum polaronic carrier densities for P3HT, with respect to the site size (ie. delocalization length of the polaron).

Table S1: Predicted doping level at saturation from the occupation of the density of states.

System		θ
2T	CN4	0.50813
2T	CN5	0.79936
3T	CN3	0.31641
3T	CN4	0.55332
3T	CN5	0.84773
4T	CN3	0.53622
4T	CN4	0.81052
4T	CN5	0.93859
P3HT	CN3	0.53147
P3HT	CN4	0.73378
P3HT	CN5	0.89341

Saturated doping levels from the Gaussian DOS model

Langmuir Isotherm Fits

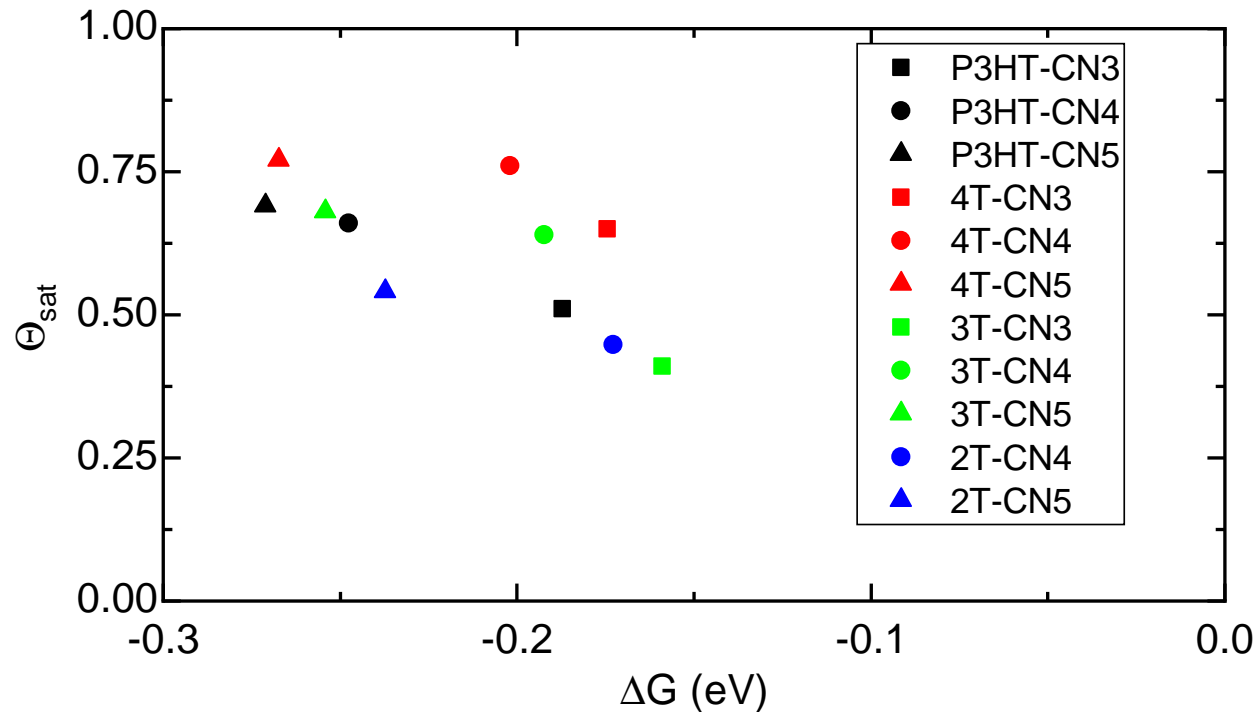


Figure S10: Experimental saturated polaron mole fraction and Gibbs Free Energy obtained from the Langmuir Isotherm Fit.

Supplemental Conductivity and Mobility

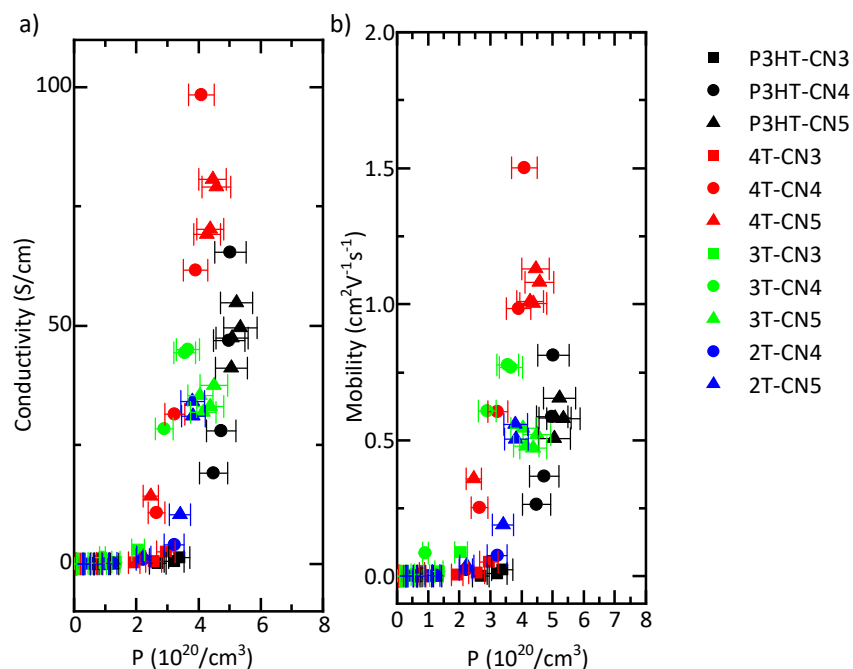


Figure S11: Conductivity and Mobility data from Figure 5 c and d plotted on a linear scale.

References

- (1) Wang, C.; Duong, D. T.; Vandewal, K.; Rivnay, J.; Salleo, A. Optical measurement of doping efficiency in poly (3-hexylthiophene) solutions and thin films. *Phys. Rev. B* **2015**, *91*, 085205.
- (2) Moulé, A. J.; Gonel, G.; Murrey, T. L.; Ghosh, R.; Saska, J.; Shevchenko, N. E.; Denti, I.; Ferguson, A. S.; Talbot, R. M.; Yacoub, N. L.; Mascali, M.; Salleo, A.; Spano, F. C. Quantifying Polaron Mole Fractions and Interpreting Spectral Changes in Molecularly Doped Conjugated Polymers. *Advanced Electronic Materials* **2022**, *8*, 2100888.
- (3) Saska, J.; Shevchenko, N. E.; Gonel, G.; Bedolla-Valdez, Z. I.; Talbot, R. M.; Moulé, A. J.; Mascali, M. Synthesis and characterization of solution processable, high electron affinity molecular dopants. *J. Mater. Chem. C* **2021**, *9*, 15990–15997.

- (4) Wegner, B.; Grubert, L.; Dennis, C.; Opitz, A.; Röttger, A.; Zhang, Y.; Barlow, S.; Marder, S. R.; Hecht, S.; Müllen, K.; Koch, N. Predicting the yield of ion pair formation in molecular electrical doping: redox-potentials versus ionization energy/electron affinity. *J. Mater. Chem. C* **2019**, *7*, 13839–13848.